Generation and transfer of single photons on a photonic crystal chip

Dirk Englund, Andrei Faraon, Bingyang Zhang, Yoshihisa Yamamoto, and Jelena Vučković

Ginzton Laboratory, Stanford University, Stanford CA 94305

Abstract: We present a basic building block of a quantum network consisting of a quantum dot coupled to a source cavity, which in turn is coupled to a target cavity via a waveguide. The single photon emission from the high-Q/V source cavity is characterized by twelve-fold spontaneous emission (SE) rate enhancement, SE coupling efficiency $\beta \sim 0.98$ into the source cavity mode, and mean wavepacket indistinguishability of $\sim$67%. Single photons are efficiently transferred into the target cavity via the waveguide, with a target/source field intensity ratio of 0.12 ± 0.01. This system shows great promise as a building block of future on-chip quantum information processing systems.

OCIS codes: (130) Integrated optics; (130.2790) Guided waves; (130) Integrated optics; (130.3120) Integrated optics devices; (270) Quantum Optics; (270.5580) Quantum electrodynamics; (000.1600) Classical and quantum physics; (140.3410) Laser resonators; (140.5960) Semiconductor lasers; (230) Optical devices; (230.5750) Resonators; (230.6080) Sources; (250) Optoelectronics; (250.5300) Photonic integrated circuits

References and links

1. D. Bouwmeester, J. Pan, K. Mattle, M. Eibl, H. Weinfurter, and A. Zeilinger, "Experimental quantum teleportation," Nature **390**, 575–9 (1997).
2. E. Knill, R. Laflamme, and G. J. Milburn, "A scheme for efficient quantum computation with linear optics," Nature **409**, 4652 (2001).
3. M. A. Nielsen and I. L. Chuang, *Quantum Computation and Quantum Information* (Cambridge Univ. Press, Cambridge, 2000).
4. P. Grangier, B. Sanders, and J. Vučković, "Single photons on demand," New Journal of Physics **6** (2004).
5. P. Michler, ed., *Single quantum dots: Fundamentals, Applications, and New Concepts* (Topics in Applied Physics, Springer-Verlag, 2003).
6. C. Santori, D. Fattal, J. Vučković, G. S. Solomon, and Y. Yamamoto, "Indistinguishable photons from a single-photon device," Nature **419**(6907), 594–7 (2002).
7. J. I. Cirac, P. Zoller, H. J. Kimble, and H. Mabuchi, "Quantum State Transfer and Entanglement Distribution among Distant Nodes in a Quantum Network," Phys. Rev. Lett. **78**(16), 3221–24 (1997).
8. A. Imamoğlu, D. D. Awschalom, G. Burkard, D. P. DiVincenzo, D. Loss, M. Sherwin, and A. Small, "Quantum Information Processing Using Quantum Dot Spins and Cavity QED," Phys. Rev. Lett. **83**(20), 4204–4207 (1999).
9. C. Monroe, D. M. Meekhof, B. E. King, W. M. Itano, and D. J. Wineland, "Demonstration of a Fundamental Quantum Logic Gate," Phys. Rev. Lett. **75**(25), 4714–4717 (1995).
10. J. Chiaverini, D. Leibfried, T. Schaetz, M. D. Barrett, R. B. Blakestad, J. Britton, W. M. Itano, J. D. Jost, E. Knill, C. Langer, R. Ozeri, and D. J. Wineland, "Realization of quantum error correction," Nature **432**, 602–5 (2005).
11. D. A. Fattal and Y. Yamamoto, "Single photons for quantum information processing," Ph.D. thesis, Stanford University (2005).
12. W. Yao, R. B. Liu, and L. J. Sham, "Theory of Control of the Spin-Photon Interface for Quantum Networks," Phys. Rev. Lett. **95**, 030,504 (2005).
13. B. B. Blinov, D. L. Moehring, L.-M. Duan, and C. Monroe, "Observation of entanglement between a single trapped atom and a single photon," Nature **428**, 153–7 (2004).
14. Y. Akahane, T. Asano, B.-S. Song, and S. Noda, "High-Q photonic nanocavity in a two-dimensional photonic crystal," Nature **425**, 944–947 (2003).

#80664 - $15.00 USD Received 5 Mar 2007; revised 10 Apr 2007; accepted 11 Apr 2007; published 23 Apr 2007

15. D. Englund and J. Vučković, "A direct analysis of photonic nanostructures," Opt. Express **14**(8), 3472–83 (2006).
16. E. Waks and J. Vuckovic, "Coupled mode theory for photonic crystal cavity-waveguide interaction," Opt. Express **13**, 5064–73 (2005).
17. D. Englund, D. Fattal, E. Waks, G. Solomon, B. Zhang, T. Nakaoka, Y. Arakawa, Y. Yamamoto, and J. Vučković, "Controlling the Spontaneous Emission Rate of Single Quantum Dots in a Two-Dimensional Photonic Crystal," Phys. Rev. Lett. **95**, 013,904 (2005).
18. A. Faraon, E. Waks, D. Englund, I. Fushman, and J. Vukovic, "Efficient photonic crystal cavity-waveguide couplers," Appl. Phys. Lett. **90**, 073,102 (2007).
19. A. Kiraz, M. Atatüre, and I. Imamoğlu, "Quantum-dot single-photon sources: Prospects for applications quantum-information processing," Phys. Rev. A **69**, p.032,305–1–032,305–10 (2004).
20. S. Laurent, S. Varoutsis, L. Le Gratiet, A. Lemaître, I. Sagnes, F. Raineri, A. Levenson, I. Robert-Philip, and I. Abram, "Indistinguishable single photons from a single-quantum dot in a two-dimensional photonic crystal cavity," Appl. Phys. Lett. **87**, 3107 (2005).
21. J. Vuckovic, D. Englund, D. Fattal, E. Waks, and Y. Yamamoto, "Generation and manipulation of nonclassical light using photonic crystals," Physica E Low-Dimensional Systems and Nanostructures **32**, 466–470 (2006).
22. H. N. et al., "Ultra-fast photonic crystal/quantum dot all-optical switch for future photonic networks," Opt. Express **12**, 6606–6614 (2004).

1. Introduction

Recent years have witnessed dramatic practical and theoretical advancements towards creating the basic components of quantum information processing (QIP) devices. One essential element is a source of single indistinguishable photons, which is required in quantum teleportation[1], linear-optics quantum computation[2], and several schemes for quantum cryptography [3]. Sources have been demonstrated from a variety of systems[4] including semiconductor quantum dots (QDs)[5], whose efficiency and indistinguishability can be dramatically improved by placing them inside a microcavity[6]. A second major component is a quantum channel for efficiently transferring information between spatially separated nodes of a quantum network[7]. This network would combine the ease of storing and manipulating quantum information in QDs[8], atoms or ions[9, 10], with the advantages of transferring information between nodes via photons, using coherent interfaces[11, 12, 13]. Here we demonstrate a basic building block of such a quantum network by the generation and transfer of single photons on a photonic crystal (PC) chip. A cavity-coupled QD single photon source is connected through a 25 μm channel to an otherwise identical target cavity so that different cavities may be interrogated and manipulated independently (Fig. 2). This system provides a source of single photons with a high degree of indistinguishability (mean wavepacket overlap of $\sim 67\%$), 12-fold SE rate enhancement, SE coupling factor $\beta \sim 0.98$ into the cavity mode, and high-efficiency coupling into a waveguide. These photons are transferred into the target cavity with a target/source field intensity ratio of 0.12 ± 0.01 (up to 0.49 observed in structures without coupled QDs), showing the system's potential as a fundamental component of a scalable quantum network for building on-chip quantum information processing devices.

2. Photonic network

The structure consists of two linear 3-hole defect cavities[14], butt-coupled and connected via a 25 μm-long closed portion of a waveguide (Fig. 2(a)). It was designed by component-wise Finite Difference Time Domain (FDTD) simulations in three dimensions. The waveguide design shown here supports four bands; we picked band B_{oe} to transfer light between the end-cavities (Fig. 2(b)). This band offers a wide, relatively flat spectral region of guided modes for coupling and can furthermore be confined in the high-Q end-cavities. Thanks to their near-minimum mode volume $V_{mode} \equiv (\int_V \varepsilon(\vec{r})|\vec{E}(\vec{r})|^2 d^3\vec{r}) / \max(\varepsilon(\vec{r})|\vec{E}(\vec{r})|^2) \approx 0.74(\lambda/n)^3$, these end-cavities allow a large SE rate enhancement $\propto Q/V_{mode}$.

The cavity and waveguide field decay rates can be expressed as a sum of vertical, in-plane, and material loss, respectively: $\kappa = \kappa_\perp + \kappa_{\parallel,wg} + \gamma$. Removed from the waveguide, the 'bare'

#80664 - $15.00 USD Received 5 Mar 2007; revised 10 Apr 2007; accepted 11 Apr 2007; published 23 Apr 2007

outer cavities radiate predominantly in the vertical direction at rate $\kappa_\perp$, as in-plane losses can be suppressed with enough PC confinement layers. Introducing an open waveguide coupled to the cavity creates additional loss $\kappa_{\parallel,wg}$.

In a waveguide of finite extent, the continuum of modes in the waveguide band breaks up into discrete resonances. For photon transfer, one of these must be coupled to the outer cavities. Assuming the two cavities are spectrally matched and detuned from the waveguide resonance by Δ, and that material losses γ are negligible [15], the field amplitudes in the source and target cavities (S,T) and waveguide (W) evolve according to:

$$\begin{aligned} \dot{c_s}(t) &= -i\kappa_\parallel c_w(t) - \kappa_\perp c_s(t) + p(t) \\ \dot{c_t}(t) &= -i\kappa_\parallel c_w(t) - \kappa_\perp c_t(t) \\ \dot{c_w}(t) &= -i\kappa_\parallel c_s(t) - i\kappa_\parallel c_t(t) - (\kappa_W + i\Delta)c_w(t) \end{aligned} \tag{1}$$

Here we assume equal coupling rates for the outer cavities, based on their near-identical SEM images and Q values, which fall within a linewidth of each other in most structures. The constant κ_W denotes the waveguide loss rate (other than loss into the end-cavities), and $p(t)$ represents a dipole driving the source cavity. It will suffice to analyze this system in steady-state since excitation of the modes, on the order of the exciton lifetime $\tau \sim 100$ ps, occurs slowly compared to the relaxation time of the photonic network, of order $\tau = \omega/Q \sim 1$ ps for the cavity and waveguide resonances involved. Then the amplitude ratio between the S and T fields is easily solved as $c_s/c_t = 1 + \kappa_\perp(\kappa_W + i\Delta)/\kappa_\parallel^2$.

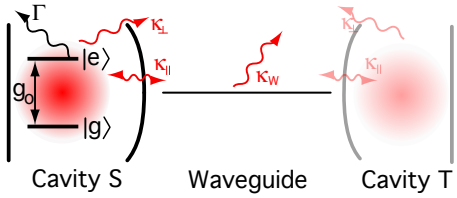

Fig. 1. Basic network consisting of two cavities and one cavity-coupled QD. The QD is coupled to a cavity (rate g_0) and decays with SE rate Γ. The cavity, in turn, is coupled to a waveguide and leaky modes at field coupling rates $\kappa_\parallel$ and $\kappa_\perp$, respectively. The waveguide field decay rate is κ_W.

In the present application, we used FDTD simulations to optimize a design with high transfer rate, while retaining high field confinement in the source cavity for enhancing the SE rate of coupled QDs. Due to computational constraints, optimization was performed for the case of a cavity connected to an open, 9-period waveguide terminated with absorbing boundary conditions (Fig. 2). The cavity resonances were targeted to a linear region of the waveguide dispersion with group velocity $V_g = 0.3c/n, n = 3.5$, slightly above the lower waveguide cut-off frequency (see Fig.2). In this way, we limited pulse dispersion and made the design more tolerant to fabrication inaccuracies. The closed-waveguide coupling constant $\kappa_\parallel$ was then calculated from the open-waveguide value $\kappa_{\parallel,wg}$ by accounting for the different densities of states in the two cases[1], giving $\kappa_\parallel/\kappa_\perp \approx 15$.

The structures were fabricated on a 160 nm-thick GaAs membrane, grown by molecular-beam epitaxy with a central layer of self-assembled InAs QDs whose photoluminesce (PL) peaks at 932 nm with an inhomogeneous linewidth of ~ 60 nm and a density of ~ 200 QDs/μm^2. The structures were fabricated by electron beam lithography and reactive ion etching, followed by a wet chemical etch to remove a sacrificial layer underneath the PC membrane[17]. Among the 30 fabricated structures, we experimentally found that fabrication

#80664 - $15.00 USD Received 5 Mar 2007; revised 10 Apr 2007; accepted 11 Apr 2007; published 23 Apr 2007

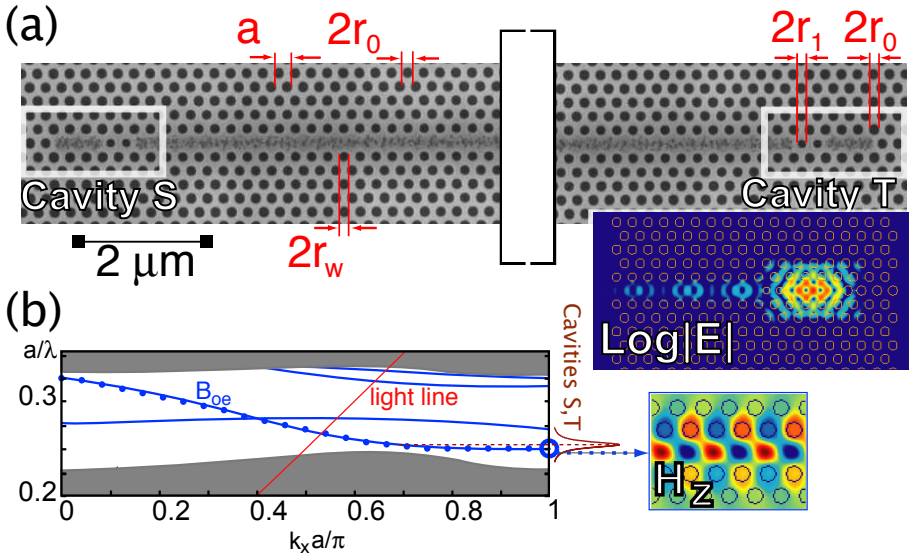

Fig. 2. Coupled cavities system. (a) The identical source (S) and target (T) cavities are connected via the 25-μm. Design parameters: PC, $a = 256$ nm, $r_0 = 0.3a$. Outer cavities, $r_1 = 0.25a, r_0 = 0.3a$. Waveguide, $r_w = 0.25a$ for the bounding rows of holes. *Inset:* Electric field pattern. (b) Waveguide dispersion diagram showing band B_{oe} used for photon transfer. The cavity resonance intersects the band's linear dispersion region just below $k_x = \pi/a$ (field pattern in inset).

inaccuracies reduced total Q values to 1560 ± 550, neglecting one outlier with $Q_s = 5100, Q_t = 4900$ for the source and target cavities.

We now focus on a particular system that showed high coupling among cavities, while also exhibiting large QD coupling in the source cavity. Measurements were done with the sample at 5K in a continuous-flow cryostat and probed with a confocal microscope setup as shown in Fig. 3. A movable aperture in the microscope image plane, together with a stir-able pump beam, allow independent adjustment of the pump and observation regions. The structures were characterized by measuring the combinations of pump/probe regions (waveguide 'WG', source cavity 'S', or target cavity 'T'). Here the broad-band PL of high-intensity, above-band pumped QDs was used as an internal illumination source. Fig. 4(a) shows good spectral match between direct measurements of the source/target cavities (plots 'SS' and 'TT'), together with the coupled emission (plots 'ST' and 'TS'). Comparison the emission intensities from S and T cavities gives the transfer efficiency $|c_t/c_s|^2 = 0.12 \pm 0.01$. This transfer occurs through one of the resonances of the terminated waveguide, which we can illuminate by pumping near the center. PL that is resonant inside the waveguide, but off-resonant from the cavities, is scattered primarily at the waveguide/cavity interfaces. On the other hand, PL that is resonant with the cavities is dropped into them and can be spatially separated with the pinhole. This drop-filtering is shown in 4(b), where the bottom plot ('WG-all') shows all modes resonant in the coupled system, while the top two plots 'WG-WG' and 'WG-T' show collection from only the waveguide terminus and the cavity, respectively. Fitting the measurements of panels (a,b) to the frequency-domain model in Eq.1 gives the coupling coefficients $\kappa_\perp = 455$ GHz, $\kappa_W = 322$ GHz, $\kappa_\parallel = 283$ GHz. The waveguide-coupling ratio $\kappa_\parallel/\kappa_\perp$ is about $24\times$ lower than expected from the simulated design. This drop is caused by fabrication errors, which primarily affect

#80664 - $15.00 USD Received 5 Mar 2007; revised 10 Apr 2007; accepted 11 Apr 2007; published 23 Apr 2007

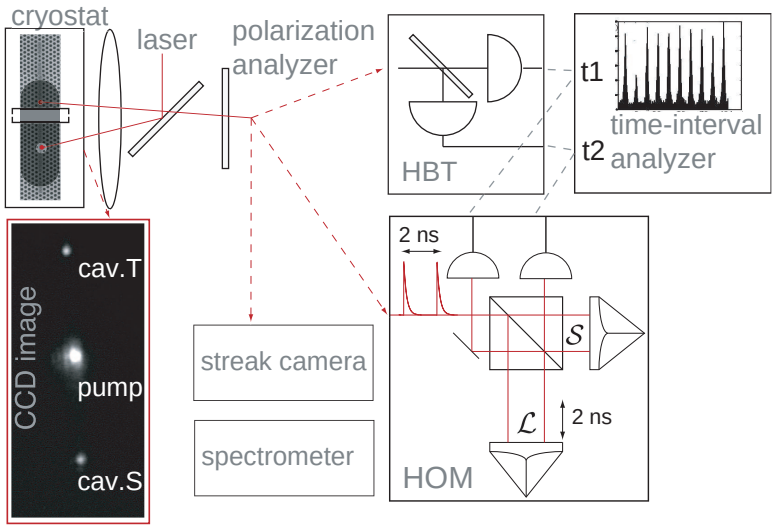

Fig. 3. Experimental setup. The sample in the He-flow cryostat is addressed with a confocal microscope with a stir-able pump beam (spot diameter ~ 1 μm) and movable probe aperture (selection region diameter 2.9 μm). PL is directed to the 0.75 m spectrometer (with LN-cooled Si detector), 0.75 m streak camera, or Hanbury-Brown-Twiss or Hong-Ou-Mandel setups. We estimate the coupling efficiency from cavity to external optics at $\sim 11\%$.

vertical confinement and lead to an 11-times higher vertical loss rate $\kappa_\perp$. Other instances of a slightly modified cavity/waveguide design, with one-hole waveguide-cavity separation, yielded photon transfer ratios as large as $|c_t/c_s|^2 = 0.49$ (Fig.6), though we did not produce this system in large enough numbers to find high cavity/QD coupling. Optimizing the geometry can improve transfer efficiency further [18]. The cavities/waveguide system strongly isolates transmission to the cavity linewidth, as seen from the transmission spectrum ('ST') (Fig. 4(c)) when S is pumped above the GaAs bandgap.

3. Network-coupled quantum dot

We now consider the problem of coupling a QD to the source cavity, which requires spatial and spectral matching. Though it primarily relies on chance, the spectral coupling can be fine-tuned by shifting the QD transitions with sample temperature. In Fig. 4(d), we show a single-excition transition coupled to cavity S at 897 nm. The transition is driven resonantly through a higher-order excited QD state with a 878 nm pump from a Ti-Saph laser. The SE rate enhancement is measured from the modified emitter lifetime, which is dominated by radiative recombination [17]. A direct streak camera measurement puts the modified lifetime at 116 ps (Fig. 5(b)). Compared to the average lifetime of 1.4 ns for QDs in the bulk semiconductor of this wafer, this corresponds to a Purcell enhancement of $F = 12$. We estimate that this value of F is about 13 times lower than for an ideally aligned dot, indicating spatial mismatch to 28% of the field maximum. The SE coupling factor into the cavity mode is then $\beta = F/(F+F_{PC}) \sim 0.98$, where $F_{PC} \sim 0.2$ reflects the averaged SE rate suppression into other modes due to the bandgap of the surrounding PC [17].

We characterized the exciton emission by measurements of the second-order coherence and indistinguishability of consecutive photons. The second-order coherence $g^{(2)}(t') = \langle I(t)I(t+t')\rangle / \langle I(t)\rangle^2$ is measured with a Hanbury-Brown and Twiss interferometer, as de-

#80664 - $15.00 USD Received 5 Mar 2007; revised 10 Apr 2007; accepted 11 Apr 2007; published 23 Apr 2007

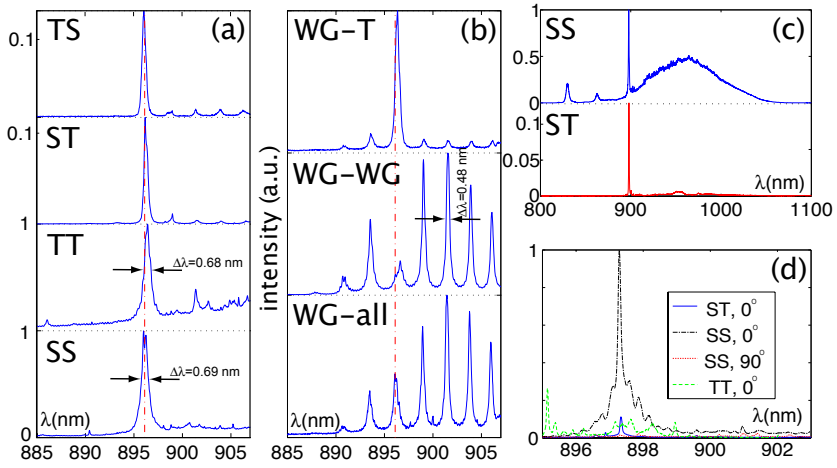

Fig. 4. Cavity-cavity coupling via a waveguide. (a) Pumping and observation from source ('S') and target ('T') cavities. (b) Cavity-coupling via a waveguide resonance. The waveguide is pumped and emission collected from the full structure ('WG-all') or spatially filtered from the waveguide ('WG-WG') or cavity T ('WG-T'). (c) Broad emission in cavity S (plot 'SS') is filtered into the target cavity (plot 'ST'). (d) When the QD exciton at 897.3 nm in cavity S is pumped (resonantly at 878 nm, 460 μW, 1μm focal spot), the emission is observed from S ('SS') and T ('ST'). The cross-polarized spectrum from S shows nearly complete quenching of QD emission ('SS, 90°'). The line at 897.3 nm is only observed when S is pumped.

scribed earlier [17]. When the QD in cavity S is pumped resonantly, then photons observed from S shows clear antibunching (Fig. 5(a)), with $g^2(0) = 0.35 \pm 0.01$. This value exceeds measurements for cavity-detuned QDs, where typically $g^{(2)}(0) < 0.05$, similar to previous reports[6]. The main contributor to the larger $g^{(2)}(0)$ for the coupled QD is enhanced background emission from nearby transitions and the wetting layer emission tail, which decays at ~ 100 ps time scales (see Fig. 5(b)) and is not completely filtered by our grating setup. The background emission is rather large in this study because of the high QD density of the sample (e.g., four times larger than that in the experiment by *Santori et al.*[6]).

Because of the shortened lifetime of the cavity-coupled QD exciton, the coherence time of emitted photons becomes dominated by radiative effects and results in high photon indistinguishability[19]. We measured the indistinguishability using the Hong-Ou-Mandel (HOM) type setup sketched in Fig. 3, similar to a recent experiment[20]. The QD is excited twice every 13 ns, with a 2.3 ns separation. The emitted photons are directed through a Michelson interferometer with a 2.3 ns time difference. The two outputs are collected with single photon counters to obtain the photon correlation histogram shown in the inset of Fig. 5(b). The five peaks around delay $\tau = 0$ correspond to the different possible coincidences on the beamsplitter of the leading and trailing photons after passing through the long or short arms $\mathscr{L}$ or $\mathscr{S}$ of the interferometer. If the two photons collide and are identical, then the bosonic symmetry of the state predicts that they must exit in the same port. This photon bunching manifests itself as *anti*-bunching in a correlation measurement on the two ports. This signature of photon indistinguishability is apparent in Fig. 5(b) in the reduced peaks near zero time delay. Following the analysis of *Santori et al.*[6], the data (inset Fig.5(b)) indicate a mean wavefunction overlap of $I = 0.67 \pm 0.18$, where we adjusted for the imperfect visibility (88%) of our setup and sub-

#80664 - $15.00 USD Received 5 Mar 2007; revised 10 Apr 2007; accepted 11 Apr 2007; published 23 Apr 2007

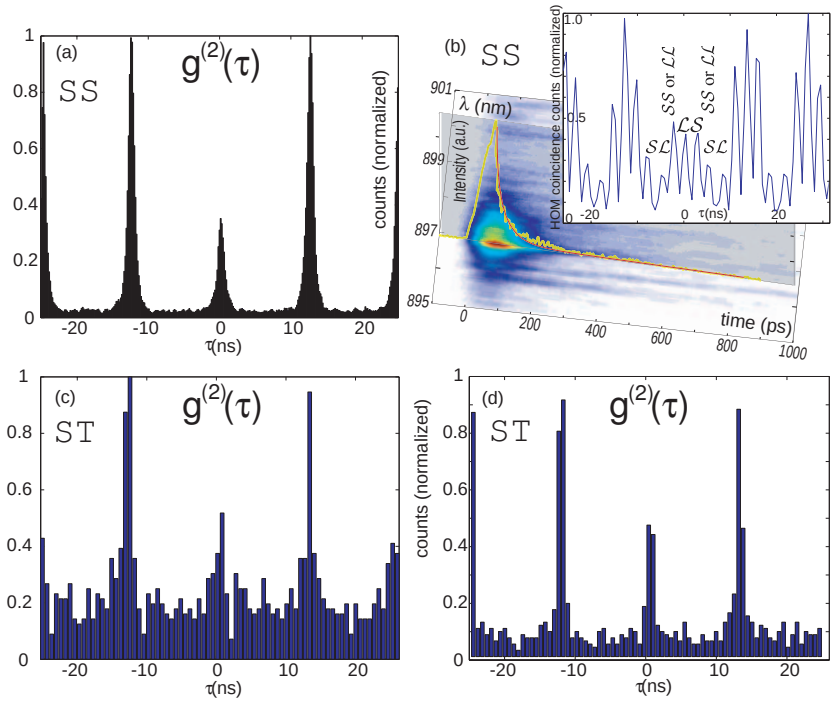

Fig. 5. Single photon source characterization. (a) Autocorrelation data when cavity S pumped and collected. (b) Streak camera data indicate exciton lifetime $\tau = 116$ ps. The rise-time is measured at 23 ps with a lower-density grating with higher time response (data not shown). *Inset:* Two-photon interference experiment (Fig.3). Colliding indistinguishable photons interfere, resulting in a decreased area of peak $\mathscr{L}\mathscr{S}$. The area does not vanish largely because of non-zero $g^{(2)}(0)$ of the source. (c) Autocorrelation data when cavity S pumped and T is collected (with grating filter). (d) Cavity S pumped and T collected directly (no grating filter).

tracted dark counts in the calculation. Even with higher SE rate enhancement, we expect that $I \lesssim 0.80$ for resonantly excited QDs[21] because of the finite relaxation time, measured here at 23 ps by the streak camera.

We will now consider the transfer of single photons to the target cavity T. The single photon transfer is described by Eqs. 1, where cavity S is now pumped by the QD single exciton. Letting $g(t), e(t)$ represent the amplitudes of states $|g, c_s = 1, c_w = 0, c_t = 0\rangle, |e, 0, 0, 0\rangle$ corresponding to the QD in the ground and excited states with one or no photons in the source cavity, we have:

$$\begin{aligned} p(t) &= -ig_0 e(t) \\ \dot{e}(t) &= -\frac{\Gamma}{2} e(t) - ig_0 g(t) \end{aligned} \tag{2}$$

Here, g_0 is the QD-field coupling strength and Γ the QD SE rate. In the present situation, where the structure's coupling rates $\kappa_\perp, \kappa_\parallel \sim 1/1$ps greatly exceed the exciton decay rate $\sim 1/116$ps, the previous steady-state results apply, and the signal from cavity T mirrors the SE of the single exciton coupled to cavity S. Experimentally, we verified photon transfer from S to T by spectral measurements as in Fig. 4(d): the exciton line is observed from T only if S is pumped. It is not visible if the waveguide or cavity T itself are pumped, indicating that this line originates from the QD coupled to cavity S and that a fraction of the emission is transferred to T. This emission has the same polarization and temperature-tuned wavelength dependence as emission

#80664 - $15.00 USD Received 5 Mar 2007; revised 10 Apr 2007; accepted 11 Apr 2007; published 23 Apr 2007

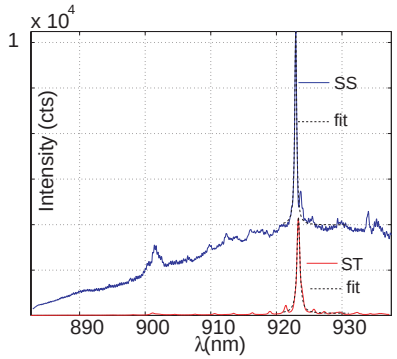

Fig. 6. The slightly modified waveguide-coupling design with a single separating hole between cavities and waveguide yields higher coupling – in this case, the S/T field intensity ratio is estimated at 0.49. No single QD was coupled to S in this structure.

from S. Photon autocorrelation measurements on the signal from T indicate the antibunching characteristic of a single emitter when S is pumped (Fig. 5(c)). The signal-to-noise ratio is rather low because autocorrelation count rates are $(|c_t/c_s|^2)^2 \sim 0.014$ times lower than for collection from S. Nevertheless, the observed antibunching does appear higher, in large part because the background emission from cavity S is additionally filtered in the transfer to T, as shown in Fig.4(b). Indeed, this filtering through the waveguide/cavity system suffices to bypass the spectrometer in the HBT setup (a 10-nm bandpass filter was used to eliminate room lights). The count rate is about three times higher while antibunching, $g^2(0) = 0.50 \pm 0.11$, is still clearly evident (Fig. 5(d)). The largest contribution to $g^2(0)$ comes from imperfectly filtered PL near the QD distribution peak seen in Fig. 4(c). This transmission appears to occur through the top of the dielectric band near $k = 0.7\pi/a$, and could easily be eliminated in the future by increasing the waveguide frequency. This on-chip filtering will be essential in future QIP applications and should also find uses in optical communications as a set of cascaded drop filters.

4. Conclusions

In conclusion, we have demonstrated a basic building block of a quantum network consisting of a QD with large coupling to a high-Q/V cavity, which in turn is coupled to a target cavity via a waveguide. We estimate that the cavity's quality factor $Q \approx 1350$ is about three times lower than that required for strong coupling between QD and cavity mode; this deficiency is due to fabrication errors and we have observed systems with sufficiently high Q values, though no coupled QDs. We currently achieve vertical-loss-limited Q values near $16,000$ in a nearly identical material, indicating that $\kappa_{\|}/\kappa_{\perp} \sim 10$ is possible through the terminated waveguide, while retaining high enough $Q > 5000$ for strong coupling. Improved PC fabrication promises to improve these figures considerably, as it has in other material systems [22]. The coupled system functions as an efficient on-demand source of single photons with mean wavepacket overlap of $\sim 67\%$, SE coupling efficiency $\beta \sim 0.98$ into the cavity mode, and high out-coupling efficiency into the waveguide. These single photons from cavity S are channeled to the target cavity, as confirmed by localized spectroscopic measurements. We measured photon transfer with a field intensity ratio of 0.12 ± 0.01 for this system. In other structures we measured field ratios up to 0.49 ± 0.04, though without coupled QDs. These efficiencies greatly exceed what is possible in off-chip transfer from a cryostat-mounted PC structure and demonstrate the great potential of this system as a building block of future on-chip quantum information processing

#80664 - $15.00 USD Received 5 Mar 2007; revised 10 Apr 2007; accepted 11 Apr 2007; published 23 Apr 2007

systems.

Acknowledgments

Financial support was provided by the MURI Center for photonic quantum information systems (ARO/DTO Program DAAD19-03-1-0199) and NSF grants ECS-0424080 & ECS-0421483. D.E. was supported by NDSEG, B. Zhang by JST. We thank David Fattal and Edo Waks for helpful discussions.

Notes

[1]Following the analysis in [16], we obtained $\kappa_{\parallel}/\kappa_{\perp} = \omega_c(v_g\kappa_{\parallel,wg}/2\pi c\kappa_{\perp}^2)^{1/2}$, using normalized FDTD program units with $\omega = 2\pi c/\lambda \approx 0.078, a/\lambda = 0.25, a = 20, c = 1$. The open-waveguide FDTD simulations give the loss rates from the out-of-plane and in-plane quality factors $Q_{\perp} \equiv \omega/2\kappa_{\perp} = 23000, Q_{\parallel,wg} \equiv \omega/2\kappa_{\parallel,wg} = 5200$.

#80664 - $15.00 USD Received 5 Mar 2007; revised 10 Apr 2007; accepted 11 Apr 2007; published 23 Apr 2007